Received: 3 November 2016 | Revised: 7 November 2017 | Accepted: 11 April 2018

DOI: 10.1002/stc.2194

RESEARCH ARTICLE

WILEY

A procedure for the identification of multiple cracks on beams and frames by static measurements

S. Caddemi[1] | I. Caliò[1] | F. Cannizzaro[1] | A. Morassi[2]

[1]Dipartimento di Ingegneria Civile e Architettura, Università di Catania, Catania, Italy

[2]Dipartimento Politecnico di Ingegneria e Architettura, Università di Udine, Udine, Italy

Correspondence
Salvatore Caddemi, Dipartimento di Ingegneria Civile e Architettura, Università di Catania, Catania, Italy.
Email: scaddemi@dica.unict.it

Funding information
Ministero dell'Istruzione, dell'Università e della Ricerca, Grant/Award Number: National Research Project PRIN 2015JW9NJT "Advanced mechanical modeling of new materials and structures for the solution of 2020 Horizon challenges"; National Research Project PRIN 2015TTJN95 "Identification and monitoring of complex structural systems"

Summary

In this work, a model of the Euler–Bernoulli beam in presence of multiple-concentrated open cracks, based on the adoption of a localized flexibility model, is adopted. The closed-form solution in terms of transversal displacements due to static loads and general boundary condition is exploited to propose an inverse damage identification procedure. The proposed identification procedure does not require any solution algorithm, on the contrary is formulated by means of simple explicit sequential expressions for the crack positions and intensities including the identification of the integration constants. The number of possible detected cracks depends on the couples of adopted sensors. Undamaged beam zones can also be easily detected in relation to the sensor positions. The analytical character of the explicit expressions of the identification procedure makes the inverse formulation applicable to damaged beams included in more complex frame structures.

The proposed procedure is applied for the identification of the number, position, and intensity of the cracks along simple straight beams and also to more complex frame structures with the aim of showing its simplicity for engineering applications. In addition, the robustness of the methodology here described is shown through an accurate analysis of the basic assumptions on which the theory relies and by means of a study of the effect of noise on the identification results.

KEYWORDS

beams, damage identification, frames, inverse problems, multiple cracks, static tests

1 | INTRODUCTION

In the literature of the last decades, the problem of damage identification, on the basis of nondestructive testing, has been the object of several studies in view of its applicability to those cases in which a simple visual inspection of the damaged structural element is not sufficient. Execution of nondestructive tests in dynamic regime provides, in general, a large number of information; however, in cases of simple structural systems, such as straight beams subject to damage, static tests are easily executable and can provide additional information to dynamic identification.

The damage identification procedures based on measurements of response parameters by nondestructive tests do not usually provide explicit solutions of the inverse, and they usually rely on numerical methods. Only recently, the problem of identification of single and multiple open cracks, modeled as linear rotational springs in single-span straight beams, has been solved by means of explicit solutions, dependent on static measurements, of damage-induced variations

in the deflection of the beam.[1,2] A careful analysis of the explicit solutions provided by the latter studies allowed the formulation of sufficient conditions on the position of the displacement measurements, for determination of both damage locations and severities.

A different line of research to deal with cracks can be followed by modeling the equivalent rotational springs by making use of distributions (generalized functions).[3,4] According to the latter approach, cracks can be modeled as Dirac's deltas in the flexural stiffness function of the beam leading to closed-form expressions in stability and dynamics of craked beams.[5,6] The latter closed-form expressions of the direct problem have been also successfully employed for the analysis of multicracked frames.[7–9] The generalized function approach has been employed for the damage identification in beam-like structures in a dynamic context.[10] Although the use of dynamic measurements for damage identification purposes is quite common in the literature[11–17] in view of the easy repeatability of the dynamic tests during the operational life, in the literature, few studies adopt a strategy based on data from static tests. In the pioneering study by Sanayei and Onipede,[18] an analytical method that makes use of static data test is employed to assess the damage in frames. More recently, regarding the static identification of damage parameters in structures, further studies were devoted to propose an alternative strategy for frames,[19] to assess instrumental errors with reference to beam-like structures,[20] to the identification of damage in arches,[21] to the identification of diffuse damage in beam-like structures[22] and to the identification of multiple concentrated cracks in beams by making use of evolutionary algorithms for the optimization procedure.[23]

In this paper, by utilizing the solution provided by the mentioned distributional approach, a further contribution towards the identification of multiple cracks in straight beams by static response measurements, leading to explicit expressions for damage positions and severities, is provided. In particular, the explicit solution of a multicracked beam is first presented as dependent on four integration constants, related to the boundary conditions (b.c.), and on summation terms showing a sequential appearance of the intensity and position crack influence on the static deflection of the beam. Then the above character of the solution is exploited for identification purposes by identifying the integration constants, first, in the region of the beam not influenced by the cracks, successively, by triggering a cascade identification of a single crack at a time in each monitored segment of the beam.

The advantage of the proposed procedure, based on the acquisition of displacement measurements by static tests along a grid of points, is that for each couple of measurements, the position and severity of a single damage, along a specified portion of the beam, can be identified by means of explicit expressions.

The methodology benefits of several properties preventing the propagation of errors and helping to recognize the violation of the basic assumption on which it relies. In addition, the sensitivity of the identified parameters is investigated with reference to both proportional and absolute noise.

Finally, the proposed damage identification procedure can be applied to any b.c., henceforth leads itself to applications for identification of cracks occurring in frame structures as also shown in the last part of the paper.

2 | A LOCALIZED FLEXIBILITY MODEL FOR A MULTICRACKED EULER–BERNOULLI BEAM

In this section, a model for the evaluation of the influence of cracks on straight beams is briefly recalled. In particular, the model makes use of generalized functions and, in the case of uniform beams, leads to explicit closed-form solutions to be exploited for identification purposes.

Localized flexibility models (LFMs) are often used to represent the behavior of damaged beams and frames. In the case of beams under plane flexural deformation, a notch or an open crack is modeled by inserting a massless rotational elastic spring at the damaged cross section.[24–33] Linear fracture mechanics arguments are usually adopted to describe (open) cracks in beams.[34] Recently, Caddemi and Morassi proposed a different justification of the rotational elastic spring model of an open crack or notch in a beam.[35] In the latter work, the authors proved that this LFM is the variational limit of a family of one-dimensional beams when the flexural stiffness of these beams tends to zero in an interval centered at the cracked cross section, and simultaneously, the length of the interval vanishes in a suitable way. In the same paper, the accuracy of the LFM has been evaluated on the basis of a series of vibration tests carried out on steel beams with single notch or multiple notches. Experimental results show that the accuracy of the LFM is comparable with that of the classical Euler–Bernoulli model for a beam without defects.

Following the approach in Caddemi and Morassi,[35] the equilibrium problem is here formulated for a beam with n cracks.

A beam of length L and bending stiffness E_oI_o = constant, subjected to a transversal load $q(x)$, x being the spatial abscissa running from 0 to L, is considered. The cracks are located at points of abscissa $x_i, \quad i = 1, ..., n$, with $0 < x_1 < x_2 < ... < x_n < \mathrm{L}$, and are modeled by rotational elastic springs of stiffness $k_i, \quad i = 1, ..., n$. The stiffness $k_i, \quad i = 1, ..., n$, depends on the geometry of the defect. Values of k_i for simple geometry of the cracked cross section are available in the literature; see, for example, Paipetis and Dimarogonas[31] and Freund and Hermann.[34]

The transverse deflection of the beam axis is governed by the following differential equation:

$$u^{(4)}(x) = \frac{q(x)}{E_oI_o} - \sum_{i=1}^{n} \frac{M(x_i)}{k_i} \delta^{(2)}(x - x_i) \tag{1}$$

under suitable end conditions at $x = 0$ and $x = L$. In the above expression, $M(x_i) = -E_oI_o\, u^{(2)}(x_i)$ is the (continuous) bending moment acting at $x = x_i$, where the superscript (k) indicates the kth derivative with respect to x and $\delta(x - x_i)$ is the Dirac's delta with support at $x = x_i$. Here, $u^{(k)(x)}$ is the kth derivative of $u(x)$.

In Caddemi and Morassi,[35] it was shown the integration procedure of Equation 1 for the case of clamped–clamped b.c. Integration of Equation 1 for any b.c. leads to the following closed-form expression of the transversal displacement function $u(x)$:

$$\begin{aligned} u(x) = c_1 + c_2 x + c_3 \left[x^2 + 2\sum_{i=1}^{n} \lambda_i (x - x_i) U(x - x_i) \right] + c_4 \left[x^3 + 6\sum_{i=1}^{n} \lambda_i x_i (x - x_i) U(x - x_i) \right] \\ + \frac{q^{[4]}(x)}{E_oI_o} + \sum_{i=1}^{n} \lambda_i \frac{q^{[2]}(x_i)}{E_oI_o} (x - x_i) U(x - x_i), \end{aligned} \tag{2}$$

where $U(x - x_i)$ is the Heaviside's, unit step, distribution with support (x_i, ∞). Here, $q^{[k]}(x)$ indicates the kth primitive function of the external load $q(x)$, namely, $q^{[1]}(x) = \int_0^x q(s_1) ds_1$, $q^{[2]}(x) = \int_0^x \int_0^{s_1} q(s_2) ds_2 ds_1$, and so on. The parameters $\lambda_i, \quad i = 1, ..., n$, appearing in the summation terms in Equation 2, represent the compliance of the rotational springs equivalent to the n cracks related to the stiffness $k_i, \quad i = 1, ..., n$, as follows: $\lambda_i = \frac{E_oI_o}{k_iL}$.

Equation 2 is the solution of a beam with multiple-concentrated open cracks dependent on four integration constants c_1, c_2, c_3, c_4 to be determined by means of the b.c. at $x = 0$ and $x = L$, without enforcement of any continuity conditions at the cracked cross sections.

Equation 2 will be exploited in this work to analyze beams with elastic end constraints also able to represent the case of damaged beams embedded in frame structures.

3 | THE IDENTIFICATION PROCEDURE OF MULTIPLE CRACKS

The great advantage of proposing multiple damage identification procedures has been addressed in Caddemi and Morassi[1,2] where explicit solutions have been also proposed on the basis of measurements by static tests.

In this work, by following a different strategy, the explicit expression of the static deflection function, given by Equation 2, is adopted to propose a novel procedure for the identification of both position and intensity of multiple cracks.

The damage identification strategy proposed in this work is based on the following *statement*:

- The transversal displacement $u(x)$ provided by Equation 2, except for the integration constants c_1, c_2, c_3, c_4, depends on the intensity and position of the cracks located at $x_i < x$ as evidenced by the terms involving the Heaviside's functions, because $U(x - x_i) = 0$, for $x < x_i$, and $U(x - x_i) = 1$, for $x > x_i$.

The property of the solution in Equation 2 reported in the above statement suggests, starting from the first damage, to employ two displacement measurements to recognize whether there is a damage on the left of the measurement position and activate a sequential identification procedure. More precisely, for each beam interval where a single damage occurs, by making use of the analytical expression given by Equation 2, evaluated at two different cross sections, it is possible to provide closed-form expressions of the crack position and intensity as functions of the measured static transversal displacements of the beam.

The above sequential identification procedure requires an a priori identification of the integration constants c_1, c_2, c_3, c_4 necessary to initiate the crack detection of a single crack in turn.

In Sections 3.1 and 3.2, devoted to beams with elastic end constraints, the procedure to identify the integration constants and the generic crack, starting from the first, respectively, are proposed in detail.

3.1 | Identification of the integration constants

In direct analysis problems, the integration constants c_1, c_2, c_3, c_4, appearing in Equation 2, can be evaluated by imposing four b.c. at both ends on the beam. The relevant expressions are generally explicitly dependent on the cracks occurring along the beam span.

However, for multicrack detection purposes, because the crack positions and intensities are unknown, the adoption the standard b.c.-dependent expressions would imply difficulties in the formulation of the inverse identification problem. For the latter reason, an analytical procedure for the identification of the integration constants derived by four additional transversal displacement values, measured by static tests at cross sections other than $x = 0,\ \ x = L$, is proposed in this subsection. The general case of beams with multiple cracks and elastic end constraints will be treated in what follows.

Precisely, for the case of a beam with elastic end constraints and a generic transversal external distributed load $q(x)$, four experimental static deflection measurements at the abscissae $x_{mo}, x'_{mo}, x''_{mo}, x'''_{mo}$, under the hypothesis that $x_{mo} < x'_{mo} < x''_{mo} < x'''_{mo} < x_1$ (as depicted in the sensor layout reported Figure 1), are here employed for the identification of the integration constants c_1, c_2, c_3, c_4.

In view of the closed-form solution given by Equation 2 and on the account of the statement asserted in the previous section, the deflection function at $x_{mo}, x'_{mo}, x''_{mo}, x'''_{mo}$ is dependent on the integration constants only. Equating the theoretical displacements $u^{th}(x_{mo}), u^{th}(x'_{mo}), u^{th}(x''_{mo}), u^{th}(x'''_{mo})$, given by Equation 2, to the experimental measurements $u^{ex}(x_{mo}), u^{ex}(x'_{mo}), u^{ex}(x''_{mo}), u^{ex}(x'''_{mo})$, as

$$\begin{aligned} u^{ex}(x_{mo}) &= u^{th}(x_{mo}; c_1, c_2, c_3, c_4), \\ u^{ex}(x'_{mo}) &= u^{th}(x'_{mo}; c_1, c_2, c_3, c_4), \\ u^{ex}(x''_{mo}) &= u^{th}(x''_{mo}; c_1, c_2, c_3, c_4), \\ u^{ex}(x'''_{mo}) &= u^{th}(x'''_{mo}; c_1, c_2, c_3, c_4), \end{aligned} \tag{3}$$

provides a system of equations to be solved with respect to c_1, c_2, c_3, c_4.

Equation 3, in view of Equation 2, can also be written explicitly as follows:

$$\begin{aligned} u^{ex}(x_{mo}) &= c_1 + c_2 x_{mo} + c_3 x_{mo}^2 + c_4 x_{mo}^3 + \frac{q^{[4]}(x_{mo})}{E_o I_o}, \\ u^{ex}(x'_{mo}) &= c_1 + c_2 x'_{mo} + c_3 x'^2_{mo} + c_4 x'^3_{mo} + \frac{q^{[4]}(x'_{mo})}{E_o I_o}, \\ u^{ex}(x''_{mo}) &= c_1 + c_2 x''_{mo} + c_3 x''^2_{mo} + c_4 x''^3_{mo} + \frac{q^{[4]}(x''_{mo})}{E_o I_o}, \\ u^{ex}(x'''_{mo}) &= c_1 + c_2 x'''_{mo} + c_3 x'''^2_{mo} + c_4 x'''^3_{mo} + \frac{q^{[4]}(x'''_{mo})}{E_o I_o}. \end{aligned} \tag{4}$$

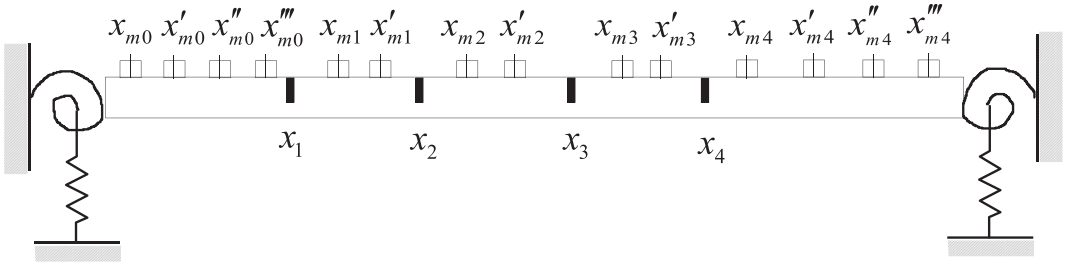

FIGURE 1 Measurement layout along a beam with multiple cracks and deformable end constraints

The matrix of the linear system in Equation 4 is of Vandermonde type. Therefore, its solution is unique, and the integration constants c_1, c_2, c_3, c_4 have the following explicit expressions:

$$
\begin{aligned}
c_1 &= -\frac{x'_{mo}x''_{mo}x'''_{mo}}{d_1}\left[u^{ex}(x_{mo})-\frac{q^{[4]}(x_{mo})}{E_oI_o}\right]+\frac{x_{mo}x''_{mo}x'''_{mo}}{d_2}\left[u^{ex}\left(x'_{mo}\right)-\frac{q^{[4]}\left(x'_{mo}\right)}{E_oI_o}\right]+\\
&\quad -\frac{x_{mo}x'_{mo}x'''_{mo}}{d_3}\left[u^{ex}\left(x''_{mo}\right)-\frac{q^{[4]}\left(x''_{mo}\right)}{E_oI_o}\right]+\frac{x_{mo}x'_{mo}x''_{mo}}{d_4}\left[u^{ex}\left(x'''_{mo}\right)-\frac{q^{[4]}\left(x'''_{mo}\right)}{E_oI_o}\right],\\
c_2 &= \frac{x'_{mo}x''_{mo}+x'_{mo}x'''_{mo}+x''_{mo}x'''_{mo}}{d_1}\left[u^{ex}(x_{mo})-\frac{q^{[4]}(x_{mo})}{E_oI_o}\right]-\frac{x_{mo}x''_{mo}+x_{mo}x'''_{mo}+x''_{mo}x'''_{mo}}{d_2}\left[u^{ex}\left(x'_{mo}\right)-\frac{q^{[4]}\left(x'_{mo}\right)}{E_oI_o}\right]+\\
&\quad +\frac{x_{mo}x'_{mo}+x_{mo}x'''_{mo}+x'_{mo}x'''_{mo}}{d_3}\left[u^{ex}\left(x''_{mo}\right)-\frac{q^{[4]}\left(x''_{mo}\right)}{E_oI_o}\right]-\frac{x_{mo}x'_{mo}+x_{mo}x''_{mo}+x'_{mo}x''_{mo}}{d_4}\left[u^{ex}\left(x'''_{mo}\right)-\frac{q^{[4]}\left(x'''_{mo}\right)}{E_oI_o}\right],\\
c_3 &= -\frac{x'_{mo}+x''_{mo}+x'''_{mo}}{d_1}\left[u^{ex}(x_{mo})-\frac{q^{[4]}(x_{mo})}{E_oI_o}\right]+\frac{x_{mo}+x''_{mo}+x'''_{mo}}{d_2}\left[u^{ex}\left(x'_{mo}\right)-\frac{q^{[4]}\left(x'_{mo}\right)}{E_oI_o}\right]+\\
&\quad -\frac{x_{mo}+x'_{mo}+x'''_{mo}}{d_3}\left[u^{ex}\left(x''_{mo}\right)-\frac{q^{[4]}\left(x''_{mo}\right)}{E_oI_o}\right]+\frac{x_{mo}+x'_{mo}+x''_{mo}}{d_4}\left[u^{ex}\left(x'''_{mo}\right)-\frac{q^{[4]}\left(x'''_{mo}\right)}{E_oI_o}\right],\\
c_4 &= \frac{1}{d_1}\left[u^{ex}(x_{mo})-\frac{q^{[4]}(x_{mo})}{E_oI_o}\right]-\frac{1}{d_2}\left[u^{ex}\left(x'_{mo}\right)-\frac{q^{[4]}\left(x'_{mo}\right)}{E_oI_o}\right]+\frac{1}{d_3}\left[u^{ex}\left(x''_{mo}\right)-\frac{q^{[4]}\left(x''_{mo}\right)}{E_oI_o}\right]-\frac{1}{d_4}\left[u^{ex}\left(x'''_{mo}\right)-\frac{q^{[4]}\left(x'''_{mo}\right)}{E_oI_o}\right],
\end{aligned}
\tag{5}
$$

where

$$
\begin{aligned}
d_1 &= x_{mo}x'_{mo}x''_{mo}-x'_{mo}x''_{mo}x'''_{mo}-x^2_{mo}x'_{mo}+x_{mo}x'_{mo}x'''_{mo}-x^2_{mo}x''_{mo}+x_{mo}x''_{mo}x'''_{mo}+x^3_{mo}-x^2_{mo}x'''_{mo},\\
d_2 &= -x_{mo}x'_{mo}x''_{mo}+x_{mo}x''_{mo}x'''_{mo}+x'^2_{mo}x_{mo}-x_{mo}x'_{mo}x'''_{mo}+x'^2_{mo}x''_{mo}-x'_{mo}x''_{mo}x'''_{mo}-x'^3_{mo}+x'^2_{mo}x'''_{mo},\\
d_3 &= -x_{mo}x'_{mo}x'''_{mo}+x_{mo}x'_{mo}x''_{mo}-x''^2_{mo}x_{mo}+x_{mo}x''_{mo}x'''_{mo}-x''^2_{mo}x'_{mo}+x'_{mo}x''_{mo}x'''_{mo}+x''^3_{mo}-x''^2_{mo}x'''_{mo},\\
d_4 &= -x_{mo}x'_{mo}x'''_{mo}+x_{mo}x'_{mo}x''_{mo}+x'''^2_{mo}x_{mo}-x_{mo}x''_{mo}x'''_{mo}+x'''^2_{mo}x'_{mo}-x'_{mo}x''_{mo}x'''_{mo}-x'''^3_{mo}+x'''^2_{mo}x''_{mo}.
\end{aligned}
\tag{6}
$$

Equation 5 provides the explicit expressions of the unknown integration constants c_1, c_2, c_3, c_4 as determined by the experimental measurements independently of the knowledge of the cracks. The latter being the main object of the inverse identification problem.

Alternative explicit expressions for the integration constants can also be obtained by starting the outlined procedure from the right end of the beam. In that case, one would need four transversal displacement measurements between the last crack occurrence and the right external constraints as also outlined in Figure 1 for the case of four cracks.

It is worth noting that the expressions in Equation 5 are able to provide the integration constants of any specific b.c. even concerning cases of no constraints or rigid constraints, such simply supported or clamped–clamped beams.

For those static tests in which the relevant b.c. are given with certainty, the explicit expression presented in Equation 5 may assume simpler expressions, and the identification of the integration constants may require less measurements.

As an example, for the case of a simply supported beam, the b.c. at $x = 0$ imply that $u(0) = u''(0) = 0$ and the integration constants $c_1 = c_3 = 0$. The remaining integration constants c_2, c_4, according to the proposed procedure, can be identified by experimental transversal displacements measured along the beam span by a nondestructive static test at the abscissae x_{mo}, x'_{mo}, such that $x_{mo}<x'_{mo}<x_1$, according to the measurement position layout depicted in Figure 2. In fact, in view of the closed-form solution given by Equation 2, transversal displacements $u(x_{mo}), u\left(x'_{mo}\right)$ measured at x_{mo}, x'_{mo} are dependent on the integration constants only, which can hence be identified by means of the linear system in Equation 4, which is reduced for the case at hand ($c_1 = c_3 = 0$) as follows:

$$
u^{ex}(x_{mo}) = c_2x_{mo}+c_4x^3_{mo}+\frac{q^{[4]}(x_{mo})}{E_oI_o} \quad , \quad u^{ex}\left(x'_{mo}\right) = c_2x'_{mo}+c_4x'^3_{mo}+\frac{q^{[4]}\left(x'_{mo}\right)}{E_oI_o}. \tag{7}
$$

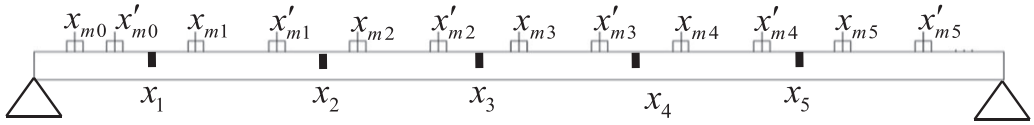

FIGURE 2 Measurement layout along a simply supported beam with multiple cracks

The solution of the linear system in Equation 7 leads to the following expressions for the identification of the integration constants c_2, c_4:

$$c_2 = \frac{1}{x_{mo}x'_{mo}} \frac{\left[u^{ex}(x_{mo}) - \frac{q^{[4]}(x_{mo})}{E_oI_o}\right]x'^3_{mo} - \left[u^{ex}(x'_{mo}) - \frac{q^{[4]}(x'_{mo})}{E_oI_o}\right]x^3_{mo}}{x'^2_{mo} - x^2_{mo}},$$
$$c_4 = \frac{1}{x_{mo}x'_{mo}} \frac{\left[u^{ex}(x'_{mo}) - \frac{q^{[4]}(x'_{mo})}{E_oI_o}\right]x_{mo} - \left[u^{ex}(x_{mo}) - \frac{q^{[4]}(x_{mo})}{E_oI_o}\right]x'_{mo}}{x'^2_{mo} - x^2_{mo}}. \tag{8}$$

Equation 8 provides the explicit expressions of the unknown integration constants c_2, c_4 as identified by the experimental measurements.

It is worth to notice that, in the latter case, in view of the a priori knowledge of the b.c., two displacement measurements have been sufficient for the identification of the integration constants.

It is worth noting that the presented procedure may be broadened to include identification of the flexural flexibility $1/E_oI_o$ with regard to those cases where the latter is not known with certainty. As a matter of example, if an additional displacement measurement at x''_{mo} denoted as $u^{ex}(x''_{mo})$ is considered, the linear system in Equation 7 can be extended as

$$\begin{aligned} u^{ex}(x_{mo}) &= c_2 x_{mo} + c_4 x^3_{mo} + \frac{q^{[4]}(x_{mo})}{E_oI_o}, \\ u^{ex}(x'_{mo}) &= c_2 x'_{mo} + c_4 x'^3_{mo} + \frac{q^{[4]}(x'_{mo})}{E_oI_o}, \\ u^{ex}(x''_{mo}) &= c_2 x''_{mo} + c_4 x''^3_{mo} + \frac{q^{[4]}(x''_{mo})}{E_oI_o} \end{aligned} \tag{9}$$

to be solved with respect to the unknowns c_2, c_4, $1/E_oI_o$ as

$$\begin{aligned} c_2 &= \frac{1}{S}\left[\begin{array}{l} x^3_{mo}q^{[4]}(x'_{mo})u^{ex}(x'_{mo}) - x'^3_{mo}q^{[4]}(x_{mo})u^{ex}(x'_{mo}) - x^3_{mo}q^{[4]}(x''_{mo})u^{ex}(x'_{mo}) + \\ + x''^3_{mo}q^{[4]}(x_{mo})u^{ex}(x'_{mo}) + x'^3_{mo}q^{[4]}(x''_{mo})u^{ex}(x_{mo}) - x''^3_{mo}q^{[4]}(x'_{mo})u^{ex}(x_{mo}) \end{array}\right], \\ c_4 &= -\frac{1}{S}\left[\begin{array}{l} x_{mo}q^{[4]}(x'_{mo})u^{ex}(x'_{mo}) - x_{mo}q^{[4]}(x''_{mo})u^{ex}(x'_{mo}) - x'_{mo}q^{[4]}(x_{mo})u^{ex}(x'_{mo}) + \\ + x'_{mo}q^{[4]}(x''_{mo})u^{ex}(x_{mo}) + x''_{mo}q^{[4]}(x_{mo})u^{ex}(x'_{mo}) - x''_{mo}q^{[4]}(x'_{mo})u^{ex}(x_{mo}) \end{array}\right], \\ \frac{1}{E_oI_o} &= \frac{1}{S}\left[\begin{array}{l} x_{mo}x'^3_{mo}u^{ex}(x'_{mo}) - x_{mo}x''^3_{mo}u^{ex}(x'_{mo}) - x'_{mo}x^3_{mo}u^{ex}(x'_{mo}) + \\ + x'_{mo}x''^3_{mo}u^{ex}(x_{mo}) + x''_{mo}x^3_{mo}u^{ex}(x'_{mo}) - x''_{mo}x'^3_{mo}u^{ex}(x_{mo}) \end{array}\right], \end{aligned} \tag{10}$$

being

$$S = x_{mo}x'^3_{mo}q^{[4]}(x''_{mo}) - x_{mo}x''^3_{mo}q^{[4]}(x'_{mo}) - x'_{mo}x^3_{mo}q^{[4]}(x''_{mo}) + x'_{mo}x''^3_{mo}q^{[4]}(x_{mo}) + x''_{mo}x^3_{mo}q^{[4]}(x'_{mo}) - x''_{mo}x'^3_{mo}q^{[4]}(x_{mo}). \tag{11}$$

3.2 | Identification of the crack positions and intensities

Once the four integration constants have been identified, Equation 2 can again be exploited to identify the first and, sequentially, the successive cracks starting from the left end of the beam.

In fact, as declared by the statement in the previous section, the theoretical expressions of transversal displacements measured at the abscissae x_{m1}, x'_{m1}, such that $x_1 < x_{m1} < x'_{m1} < x_2$, according to the sensor layout in Figures 1 and 2, are dependent on the integration constants (already identified by means of Equation 5) and on the position and intensity x_1 and λ_1, respectively, of the first crack.

Equating the theoretical displacements $u^{th}(x_{m1}), u^{th}(x'_{m1})$, given by Equation 2, to the experimental measurements $u^{ex}(x_{m1}), u^{ex}(x'_{m1})$, at the same abscissae, as

$$u^{ex}(x_{m1}) = u^{th}(x_{m1}; x_1, \lambda_1) \quad , \quad u^{ex}(x'_{m1}) = u^{th}(x'_{m1}; x_1, \lambda_1), \tag{12}$$

provides a system of equations to be solved with respect to x_1 and λ_1 for the identification of the first crack.

Equation 12 can be written explicitly as follows:

$$\begin{aligned} u^{ex}(x_{m1}) &= c_1 + c_2 x_{m1} + c_3\left[x_{m1}^2 + 2\lambda_1(x_{m1} - x_1)\right] + c_4\left[x_{m1}^3 + 6\lambda_1 x_1(x_{m1} - x_1)\right] + \frac{q^{[4]}(x_{m1})}{E_o I_o} + \lambda_1 \frac{q^{[2]}(x_1)}{E_o I_o}(x_{m1} - x_1), \\ u^{ex}(x'_{m1}) &= c_1 + c_2 x'_{m1} + c_3\left[x'^2_{m1} + 2\lambda_1(x'_{m1} - x_1)\right] + c_4\left[x'^3_{m1} + 6\lambda_1 x_1(x'_{m1} - x_1)\right] + \frac{q^{[4]}(x'_{m1})}{E_o I_o} + \lambda_1 \frac{q^{[2]}(x_1)}{E_o I_o}(x'_{m1} - x_1). \end{aligned} \tag{13}$$

By eliminating the unknown λ_1 in Equation 13, the system can be solved explicitly in terms of the crack position x_1 as

$$x_1 = \frac{x_{m1} D(x'_{m1}) - x'_{m1} D(x_{m1})}{D(x'_{m1}) - D(x_{m1})}, \tag{14}$$

where $D(x)$ is given as

$$D(x) = u^{ex}(x) - c_1 - c_2 x - c_3 x^2 - c_4 x^3 - \frac{q^{[4]}(x)}{E_o I_o} \tag{15}$$

and where it was assumed that the denominator in Equation 14 does not vanish.

Once the position x_1 of the first crack is evaluated by means of Equation 14, the first equation appearing in Equation 13 can be solved with respect to λ_1, as follows:

$$\lambda_1 = \frac{D(x_{m1})}{\left[2c_3 + 6c_4 x_1 + \frac{q^{[2]}(x_1)}{E_o I_o}\right](x_{m1} - x_1)}. \tag{16}$$

The next step of the crack identification procedure consists in the employment of the experimental transversal displacement measured at the abscissae x_{m2}, x'_{m2}, such that $x_2 < x_{m2} < x'_{m2} < x_3$ as in Figures 1 and 2, to identify the position and intensity x_2, λ_2 of the second crack.

Precisely, equating the theoretical displacements $u^{th}(x_{m2}), u^{th}(x'_{m2})$, given by Equation 2, to the experimental measurements $u^{ex}(x_{m2}), u^{ex}(x'_{m2})$, provides a system of equations to be solved with respect to x_2 and λ_2 for the identification of the second crack as follows:

$$\begin{aligned} u^{ex}(x_{m2}) &= c_1 + c_2 x_{m2} + c_3\left[x_{m2}^2 + 2\lambda_1(x_{m2} - x_1) + 2\lambda_2(x_{m2} - x_2)\right] + c_4\left[x_{m2}^3 + 6\lambda_1 x_1(x_{m2} - x_1) + 6\lambda_2 x_2(x_{m2} - x_2)\right] \\ &\quad + \frac{q^{[4]}(x_{m2})}{E_o I_o} + \frac{q^{[2]}(x_1)}{E_o I_o}\lambda_1(x_{m2} - x_1) + \frac{q^{[2]}(x_2)}{E_o I_o}\lambda_2(x_{m2} - x_2), \\ u^{ex}(x'_{m2}) &= c_1 + c_2 x'_{m2} + c_3\left[x'^2_{m2} + 2\lambda_1(x'_{m2} - x_1) + 2\lambda_2(x'_{m2} - x_2)\right] + c_4\left[x'^3_{m2} + 6\lambda_1 x_1(x'_{m2} - x_1) + 6\lambda_2 x_2(x'_{m2} - x_2)\right] \\ &\quad + \frac{q^{[4]}(x'_{m2})}{E_o I_o} + \frac{q^{[2]}(x_1)}{E_o I_o}\lambda_1(x'_{m2} - x_1) + \frac{q^{[2]}(x_2)}{E_o I_o}\lambda_2(x'_{m2} - x_2). \end{aligned} \tag{17}$$

By eliminating the unknown λ_2 in Equation 17, the system can be solved explicitly in terms of the crack position x_2 as

$$x_2 = \frac{x_{m2}\left[D\left(x'_{m2}\right) + F\left(x'_{m2}\right)\right] - x'_{m2}\left[D(x_{m2}) + F(x_{m2})\right]}{D\left(x'_{m2}\right) + F\left(x'_{m2}\right) - D(x_{m2}) - F(x_{m2})}, \tag{18}$$

where $D(x)$ is given in Equation 15, whereas $F(x)$ is given as

$$F(x) = -\lambda_1 (x - x_1)\left[\frac{q^{[2]}(x_1)}{E_o I_o} + 2c_3 + 6c_4 x_1\right], \tag{19}$$

and where it was assumed that the denominator in Equation 18 does not vanish.

Once the position x_2 of the second crack is evaluated by means of Equation 18, the first equation appearing in Equation 17 can be solved with respect to λ_2 as follows:

$$\lambda_2 = \frac{D(x_{m2}) + F(x_{m2})}{\left[2c_3 + 6x_2 c_4 + \frac{q^{[2]}(x_2)}{E_o I_o}\right](x_{m2} - x_2)}. \tag{20}$$

The procedure described so far for the identification of the first two cracks can be easily conducted sequentially for the successive cracks, according to the sensor layout depicted in Figure 1, leading to the following closed-form expressions for the position and intensity of the ith crack:

$$x_i = \frac{x_{mi}\left[D\left(x'_{mi}\right) + F\left(x'_{mi}\right)\right] - x'_{mi}\left[D(x_{mi}) + F(x_{mi})\right]}{D\left(x'_{mi}\right) + F\left(x'_{mi}\right) - D(x_{mi}) - F(x_{mi})}, \tag{21}$$

$$\lambda_i = \frac{D(x_{mi}) + F(x_{mi})}{\left[2c_3 + 6x_i c_4 + \frac{q^{[2]}(x_i)}{E_o I_o}\right](x_{mi} - x_i)}, \tag{22}$$

where $D(x)$ is given by Equation 15, whereas $F(x)$, originally provided by Equation 19, is now generalized as

$$F(x) = -\sum_{k=1}^{i-1} \lambda_k (x - x_k)\left[\frac{q^{[2]}(x_k)}{E_o I_o} + 2c_3 + 6c_4 x_k\right] \tag{23}$$

and where it was assumed that the denominator in Equation 21 does not vanish.

The proposed damage identification procedure leads to explicit expressions of the integration constants c_1, c_2, c_3, c_4 (as described in Section 3.1), the damage position x_i, and intensity λ_i. More precisely, Equation 5 provides c_1, c_2, c_3, c_4 explicitly as functions of the experimentally measured displacements $u^{ex}(x_{mo})$, $u^{ex}\left(x'_{mo}\right), u^{ex}\left(x''_{mo}\right), u^{ex}\left(x'''_{mo}\right)$, whereas Equations 21 and 22 provide x_i and λ_i, respectively, in terms of the displacements $u^{ex}(x_{mi})$, $u^{ex}\left(x'_{mi}\right)$, detected in the undamaged region between the ith and the $(i + 1)$th crack to be identified.

Equations 21 and 22, in view of Equation 23, show the dependence of the position x_i and intensity λ_i, of the ith crack, on the positions and intensities of the cracks denoted as $k = 1, \ldots, i - 1$. The latter circumstance implies that Equations 21 and 22 apply to a sequential identification of each single crack separately and allow to detect and quantify a crack along prescribed segments of the beam as indicated by the chosen sensor layout adopted in the execution of the nondestructive test.

It is worth to notice that the sequential character of the proposed procedure can be considered an advantage because it reduces the multicrack identification problem to a sequence of steps implying a single crack identification each. However, at the same time, it may also be considered a drawback due to the inevitable measurement/instrumental errors propagation through the successive steps.

An extensive study on the influence of the errors on the proposed identification procedure is however reported in the applications.

It should also be remarked that, according to the sufficient conditions involving the measurement layout indicated in Caddemi and Morassi,[1,2] a couple of measurement displacements (one at the left and one at the right of each crack) is always adopted in the experimental test as evidenced in Figures 1 and 2.

One of the advantages of the proposed procedure is that it can be stopped whenever it is desired, and the results obtained up to that point are valid. The consequence is that the number of cracks the operator intends to identify (and the region where they are sought) will indicate the number (and positions) of the sensors to be used and vice versa. The procedure provides the correct crack identification even though less cracks than the actual ones are sought. Finally, the actual number of cracks is identified when the adopted sensors stop indicating the presence of cracks.

4 | FRAME STRUCTURES COMPOSED BY DAMAGED BEAMS

The case of a beam with deformable end constraints treated in Section 3.1 allows to treat the problem of identification of multiple cracks along a beam of a complex and extended frame structure as in Figure 3. The proposed identification procedure can, in fact, be applied by testing uniquely the damaged beam of interest, the frame surrounding the beam being modeled by the unknown deformable end constraints. This is possible in view of the introduction of the integration constants c_1, c_2, c_3, c_4 in the identification process.

An example of damaged frame will be considered in the next section where measurement sensors are placed exclusively along the span of a chosen beam where multiple cracks are to be detected once the integration constants representing the surrounding frame have been identified.

It is important to notice that if the beam is constantly monitored, variations of the identified integration constants, in absence of crack growth on the monitored beam, provide crucial information on damage occurrence in the surrounding frame.

The latter use of the proposed procedure provides indication on possible damage occurrences on the overall frame by testing a restricted undamaged portion of the frame.

Because the proposed method applies to single beam elements of more complex frames, it would be time consuming if it applies to all the elements, so the method should be intended as a local method. However, a preliminary application of suitable global damage detection methods might provide indication of the possible damaged elements, to which the proposed method can be locally applied. Convenient global damage detection methods might rely on dynamic measurements, as proposed in Hao and Xia[36] and Lam and Yang.[37]

5 | NUMERICAL APPLICATIONS

In this section, two numerical examples to verify the reliability of the proposed procedure are presented. Without loss of generality in this paper for the numerical applications, the following expression of the external load will be employed

$$q(x) = q_0 + \sum_{k=1}^{n_P} P_k \, \delta\left(x - x_{P,k}\right), \tag{24}$$

which embeds a constant distributed load q_0 and n_P-concentrated loads P_k acting at $x_{P,\,k}$. The two loads can act on the beam at the same time or alternatively. However, the analytical derivations already reported are consistent whichever external load typology is adopted.

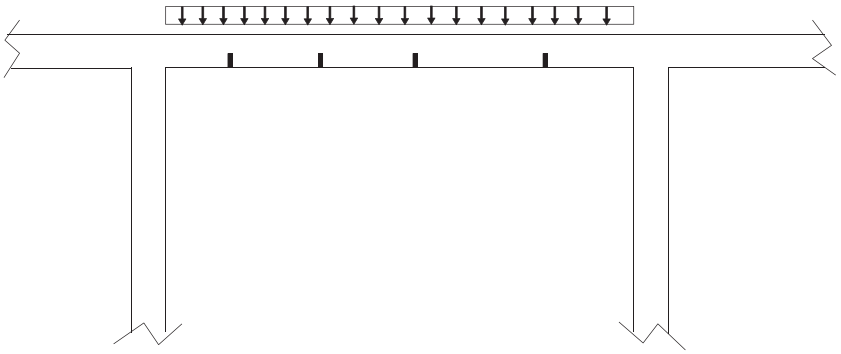

FIGURE 3 A frame structure with a damaged beam

5.1 | A simply supported beam

In this section, an application of the proposed identification procedure to a simply supported beam in presence of multiple cracks, on the basis of "experimental" displacement measurements simulated by a finite element model (FEM), is presented.

The damaged simply supported beam subjected to concentrated static loads is depicted in Figure 4, together with the measurement layout. In particular, the beam, with length $L = 2{,}000$ mm, has square steel cross section (Young's modulus $E_o = 206{,}000$ MPa) with height $h = 50$ mm. Furthermore, four cracks with depth d involving 50% of the cross-sectional height h, at abscissae $x_1 = 350$, $x_2 = 900$, $x_3 = 1{,}300$, $x_4 = 1{,}500$ mm, are present.

In accordance to the conditions, regarding the measurement positions, presented in the proposed identification procedure, measurement displacements are detected at the following cross sections:

$$
\begin{aligned}
&x_{mo} = 150\,\text{mm} < x'_{mo} = 25\,\text{mm} < x_1,\\
&x_1 < x_{m1} = 550\,\text{mm} < x'_{m1} = 650\,\text{mm} < x_2,\\
&x_2 < x_{m2} = 950\,\text{mm} < x'_{m2} = 1{,}050\,\text{mm} < x_3,\\
&x_3 < x_{m3} = 1{,}350\,\text{mm} < x'_{m3} = 1{,}450\,\text{mm} < x_4,\\
&x_4 < x_{m4} = 1{,}750\,\text{mm} < x'_{m4} = 1{,}850\,\text{mm} < L.
\end{aligned}
$$

The displacement measurements have been generated by means of a finite element plane model of the beam by making use of a 1 mm × 2 mm rectangular mesh as also shown in Figure 4.

Finally, the results of the proposed identification procedure are summarized in Table 1, where the identified values of the position and the ratios d_i/h are compared with the crack values assumed for the FEM and the relative errors are reported. The same results are also reported, in terms of graph, in Figure 5.

5.2 | Robustness of the identification procedure

The presented multicrack identification procedure relies on the assumption that each crack is located between two pairs of measurements. However, in this section, the performance of the proposed procedure will be assessed in case the mentioned basic hypothesis is removed. Precisely, two cases can be considered:

(a) absence of crack between two consecutive pairs of measurements and
(b) presence of two (or more) cracks between two consecutive pairs of measurements.

To check the robustness of the procedure under the above mentioned scenarios, the example reported in Figure 6 is considered. The beam length is equal to 4,000 mm, and the Young's modulus of the beam and the moment of inertia of

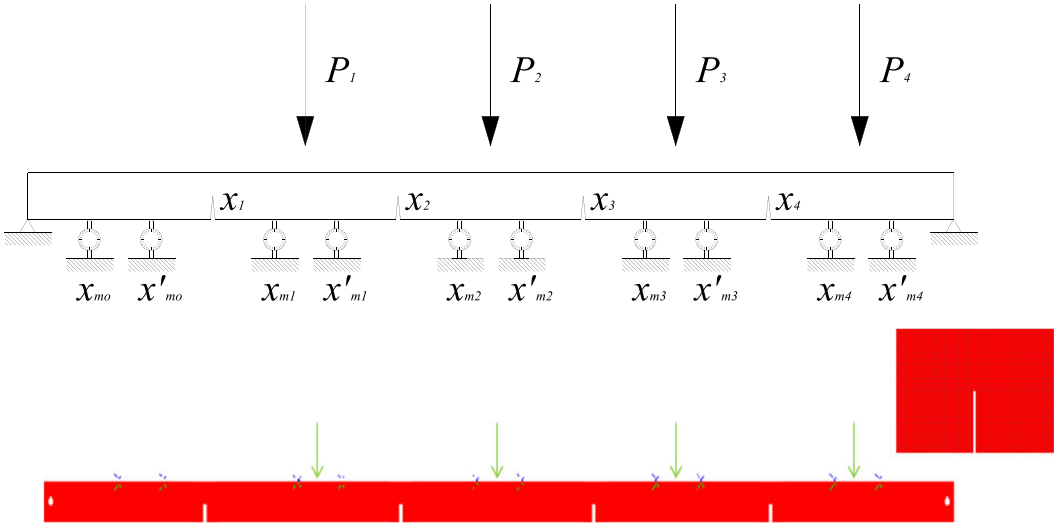

FIGURE 4 Scheme of the simply supported beam with the finite element model

TABLE 1 FEM values and identified values of the crack positions and intensities

FEM		Identified			
x_i (m)	d_i/h	x_i (m)	Error (%)	d_i/h	Error (%)
0.35	0.5	0.3506	0.17	0.5122	2.44
0.90	0.5	0.9009	0.10	0.5129	2.58
1.30	0.5	1.3000	0.00	0.5126	2.52
1.50	0.5	1.5000	0.00	0.5121	2.42

Note. FEM = finite element model.

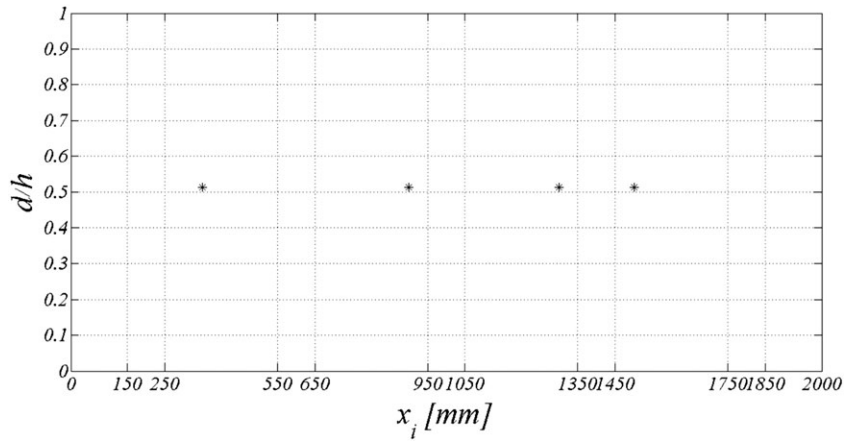

FIGURE 5 Identified values of the crack positions and intensities

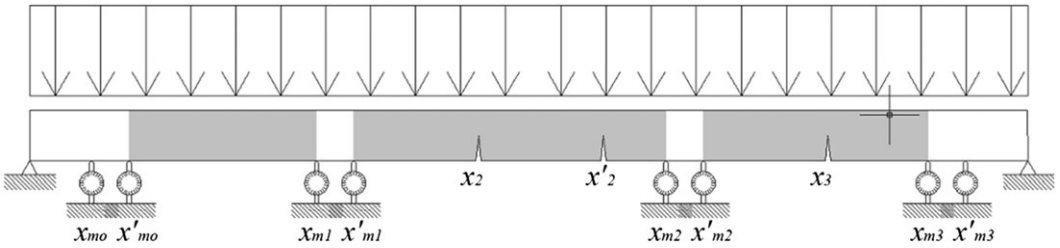

FIGURE 6 Layout of the considered cracked beam

the cross section are $E = 210{,}000$ MPa and $I = 66{,}666{,}666.66$ mm^4 ($b = 100$ mm and $h = 200$ mm), respectively. The beam is subjected to a uniform load $q = 5$ N/mm. Three cracks are located along the axis of a simply supported beam, at the abscissae $x_2 = 1{,}800$ mm, $x'_2 = 2{,}200$ mm, and $x_3 = 3{,}200$ mm. All the cracks have the same severity equal to $\lambda = 151.8738$ corresponding to a crack depth $d/h = 0.2293$.[38] Eight measurement points are located at the abscissae $x_{mo} = 250$ mm, $x'_{mo} = 400$ mm, $x_{m1} = 1{,}150$ mm, $x'_{m1} = 1{,}300$ mm, $x_{m2} = 2{,}550$ mm, $x'_{m2} = 2{,}700$ mm, $x_{m3} = 3{,}600$ mm, and $x'_{m3} = 3{,}750$ mm. Differently from the actual crack locations, the considered experimental layout implies the hypothesis of three cracks present along the axis of the beam, each of them located along one of the gray areas reported in Figure 6. In particular, the first two measurements x_{mo} and x'_{mo} will be employed to identify the integration constants, and the following three pairs of measurements x_{mi} and x'_{mi}, $i = 1, ..., 3$, will be employed to locate three cracks. The actual damage scenario corresponds to the occurrence of the above mentioned conditions (a) and (b).

By running the identification procedure, the obtained results are reported in Table 2. Some interesting comments can be made on the obtained results:

(i) When no crack is present before a pair of measurements, the proposed procedure recognizes that the identified crack has zero flexibility, that is, no crack is identified;
(ii) when two cracks are located before a pair of measurements, the proposed procedure identifies a single crack to be considered equivalent to the actual ones; and

TABLE 2 Identified values for the beam reported in Figure 6

Actual damage scenario			Identified scenario	
Crack	Location (m)	d/h	x_i (m)	d/h
x_1	—	—	—	0
x_2	1.80	0.2293	2.00	0.3481
x_2'	2.20	0.2293		
x_3	3.20	0.2293	3.20	0.2293

(iii) both the previous circumstances imply that the exact identification of the third crack is not compromised.

With regard to comment (ii), the single-identified crack is considered equivalent to the actual crack layout in view of comment (iii) that guarantees the correctness of the subsequent crack identification. In order to reconstruct the actual crack layout, the identification procedure can be applied for a couple of measurement points roving from the left end to the right end of the beam, as shown in Figure 7. Discontinuities in the identified crack position are expected as a measurement point crosses a crack.

In Figure 8, the results for the considered test scheme as in Figure 7 are reported. The application was obtained considering a mutual distance between the two roving stations equal to 150 mm. It can be noticed that, as the pair of measurements moves, the identified crack location is first equal to zero (no crack is present) and then, when the first measurement crosses the first crack, the identified crack position x_{id} exhibits a jump. As both measurements pass over the first crack, x_{id} reaches a constant value providing the location of the first crack (lowest dashed line). Generally speaking, Figure 8 shows that every time a measurement point crosses a crack, a jump in the crack location identification is encountered. According to the graph reported in Figure 8, the actual crack distribution can be correctly reconstructed.

It is important to note that the latter property enhanced by analysis of Figure 8 is encountered even for a couple of roving measurement over a restricted portion of the beam in view of comments (ii) and (iii).

The achieved results can be easily extended to a crack located in proximity of the left end of the beam. In fact, the first set of measurements is employed to identify the integration constants under the hypothesis that no crack is located on their left. However, equivalent integration constants can be identified even in presence of a crack located before the first measurement; again, the term equivalent is adopted in the sense that the identified integration

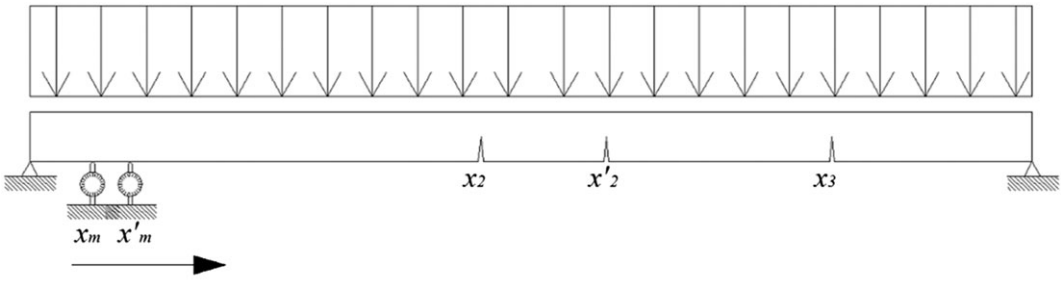

FIGURE 7 Layout of the procedure with roving measurements

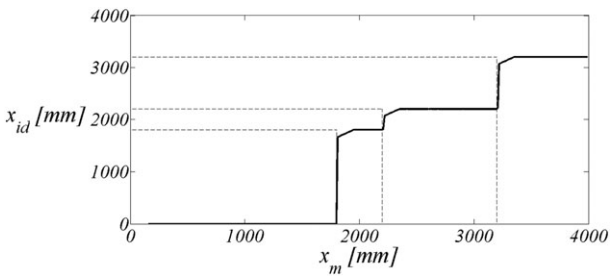

FIGURE 8 Location of the progressively identified crack

constants embed the effect of the cracks located before the first measurements and guarantee the correctness of the subsequent crack identification. Finally, if a crack is located among the measurements, this circumstance can be recognized by moving the measurements; in fact, in this case, the identified integration constants will change as the measurements move.

In case the latter procedure indicates the presence of a crack in the vicinity of the left of the beam, simultaneous identification of both the integration constants and the first crack might be pursued by modifying the algebraic system in Equation 4 or 7 by adding two equations to include the influence of crack intensity and position. Although the latter modification allows to deal with a different basic hypothesis, it implies analytical difficulties due to the nonlinearity of the resulting system.

5.3 | A damaged frame

The proposed damage identification procedure, presented in the previous section, differently from the procedures provided in the literature, includes the identification of the integration constants, and for this reason, it applies to any b.c. The latter circumstance includes the case of a damaged beam embedded in a frame structure subjected to static loads.

In this section, an application of crack identification to the damaged steel frame depicted in Figure 9 (width $L = 2{,}000$ mm, height $H = 2{,}000$ mm), to show the potentiality of the proposed procedure, is considered.

The frame has constant square cross section with height $h = 5$ cm. In particular, the beam element supported by the two columns is subjected to two cracks at abscissa $x_1 = 80$ cm and $x_2 = 120$ cm with depth d involving 50% of the cross-sectional height h and is loaded with two concentrated forces P_1, P_2 with 1,000 N intensity each.

According to the identification procedure presented in Section 3, the damaged element beam supported at the ends by two columns can be considered as a beam with unknown end constraints.

Because, in this case, the b.c. require four integration constants to be identified, according to the proposed identification procedure, four displacement measurements are needed at the left of the first damage. Hence, measurement displacements are detected along the beam span at $x_{m0} = 150\,\text{mm} < x'_{m0} = 250\,\text{mm} < x''_{m0} = 550\,\text{mm} < x'''_{m0} = 650\,\text{mm}$, for the identification of c_1, c_2, c_3, c_4; at $x_1 < x_{m1} = 950\,\text{mm} < x'_{m1} = 1{,}050\,\text{mm} < x_2$ between the first and the second cracks for the identification of the first crack; and finally at $x_2 < x_{m2} = 1{,}350\,\text{mm} < x'_{m2} = 1{,}450\,\text{mm} < L$ for the identification of the second crack. Further displacement measurements detected at $x'_{m2} < x''_{m2} = 1{,}750\,\text{mm} < x'''_{m2} = 1{,}850\,\text{mm} < L$ are redundant. However, the latter can be useful in case the sequential identification procedure is initiated from the right end $x = L$.

The displacement values of the measurement cross sections of the deformed structure, reported in Figure 10, have been generated by means of a FEM.

The damage identification procedure proposed in the previous section led to the results summarized in Table 3 and shown in the graph reported in Figure 11.

The error levels of the results obtained by means of the proposed identification procedure are also reported in Table 3 showing the validity of the procedure in presence of uncertainties due to the adopted model.

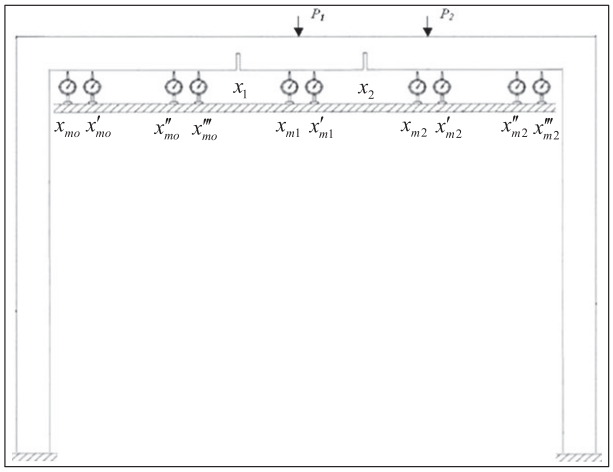

FIGURE 9 A frame with two concentrated cracks

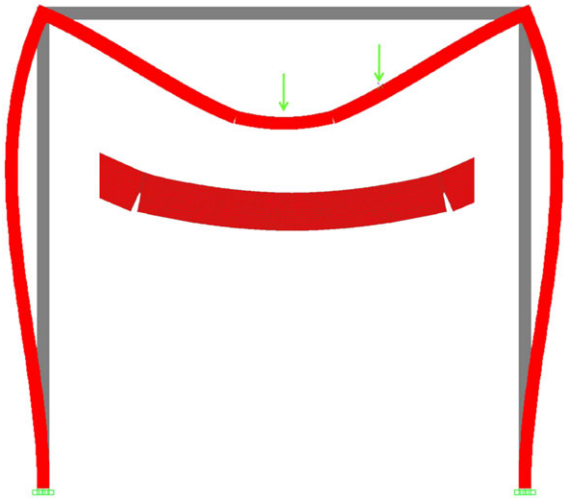

FIGURE 10 Deformed shape of the frame in Figure 9 evaluated by means of finite element model

TABLE 3 FEM values, identified values, and errors of the crack positions and intensities

	FEM	Identified	Error (%)
x_1 (m)	0.8	0.802	0.19
d_1/h	0.5	0.505	1.08
x_2 (m)	1.2	1.199	0.08
d_2/h	0.5	0.507	1.40

Note. FEM = finite element model.

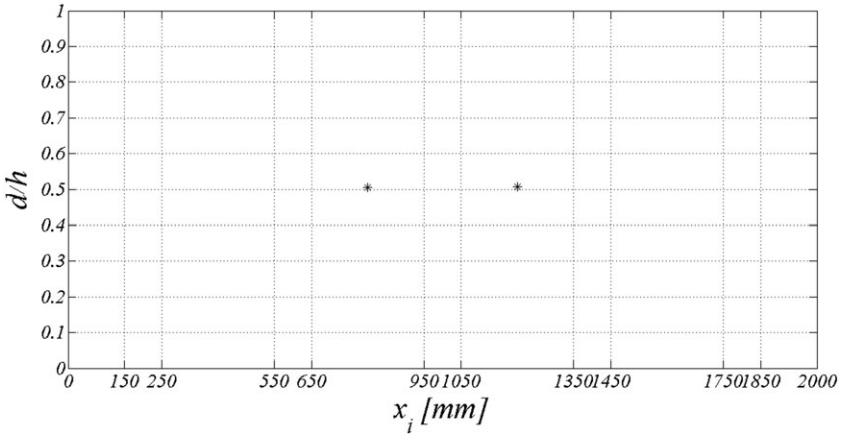

FIGURE 11 Identified values of the crack positions and intensities in the frame of Figure 9

5.4 | Crack identification in presence of noisy measurements

The following results refer to two simply supported beams with a length $L = 3{,}500$ mm and subjected to a uniform transversal load $q = 5$ N/mm (Figure 12). The Young's modulus of the beams and the moment of inertia of the cross section are $E = 210{,}000$ MPa and $I = 66{,}666{,}666.66$ mm^4 ($b = 100$ mm and $h = 200$ mm), respectively. Two damage scenarios are considered, namely, single- (Figure 12a) and double-cracked (Figure 12b) beams. Both beams have a crack located at the abscissa $x_1 = 1{,}600$ mm with a depth $\eta = d/h = 0.2293$, whose corresponding compliance $\lambda_i = 151.8738$ can be computed according to Billelo.[38] In addition, the double-cracked beam has a second crack, characterized by the same severity, located at the abscissa $x_2 = 2{,}500$ mm.

Since the beam is simply supported, two measurements are needed to assess the two unknown integration constants C_2 and C_4 (equal to 0.0071 and $-1.0417 * 10^{-9}$, respectively), and two are needed to identify each crack position and intensity.

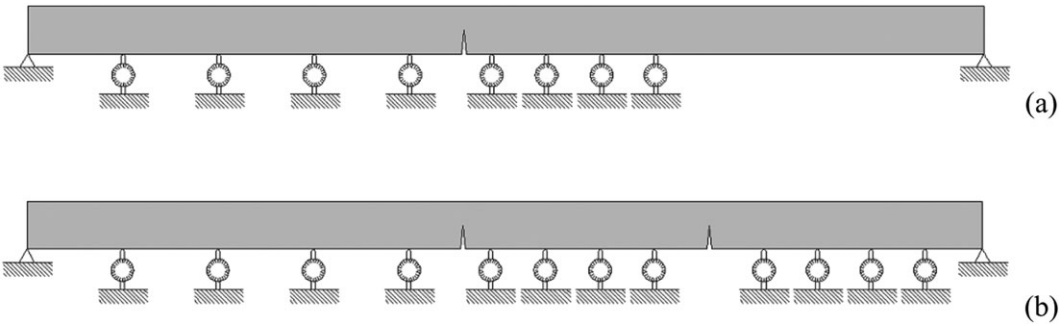

FIGURE 12 Influence of noise—layout of the test: (a) single- and (b) double-cracked beams

To assess the influence of noise on the measurements, both proportional and absolute errors are considered. The measurements adopted in the identification procedure can be computed as follows:

$$\begin{aligned} u^{ex}(x_m) &= u^c(x_m)\left(1+\varepsilon_p R\right), \\ u^{ex}(x_m) &= u^c(x_m)+\varepsilon_a R, \end{aligned} \tag{25}$$

where ε_p and ε_a are the considered proportional and absolute errors, respectively, and R represents a random variable with uniform distribution in the interval $[-1, 1]$.

To test the robustness of the procedure, the identification algorithm is repeated with increasing values of the error. Two strategies are here adopted to improve the robustness of the procedure, namely, one that employs additional measurements and one that employs additional load scenarios. The two procedures are better described and verified in the following.

5.4.1 | Crack identification employing additional measurements

This identification strategy is based on the adoption of a number of measurements higher than those strictly needed. In particular, with reference to the single-cracked beam shown in Figure 12a, besides the case where the measurements strictly needed are employed (located at the abscissae 350, 700, 1,700, and 1,900 mm), the procedure is repeated considering an increasing number of additional measurements and employing the Moore–Penrose inversion algorithm. To this purpose, two other cases are considered. In the first case, two measurements are added (located at 1,150 and 2,100 mm), and in the second, two more measurements are considered (located at 1,400 and 2,300 mm).

The sensitivity to the noise was assessed by means of Monte Carlo simulations, as reported in Figure 13 over 5,000 samples for the cases of proportional error. The average value of the crack locations and intensity over the performed runs is reported as function of the performed samples.

For the case of proportional error, Figure 13, the error has been ranged in the interval $\varepsilon_p = 0.1$–1%. The results reported in the following show how 5,000 samples are enough to converge to a stable value of the average of the identified values. It is clear how, as the error in the measurements increases, the identified values tend to distance the actual values. However, the additional measurements have a beneficial effect to limit the errors in the identification procedure.

The results previously reported, together with those relative to the absolute errors (ranged in the interval $\varepsilon_a = 10^{-3}$–10^{-2} mm, which correspond to a relative error with respect to the maximum deflection equal to 0.13–1.3%), are summarized in Figure 14 where the error in the identified values is reported as a function of the error in the measurements for the three considered cases (2, 3, and 4 measurements for each segment). In terms of relative values, the range studied for the absolute error is comparable with that adopted for the applications with proportional error. The error range adopted in the present applications appears to be comparable with respect to that encountered in the execution of real static tests.[2]

The errors for the crack position and depth are computed as follows:

$$\begin{aligned} \varepsilon(x) &= \frac{\left|x_i^r - x_i^{id}\right|}{L}, \\ \varepsilon(\eta) &= \left|\eta_i^r - \eta_i^{id}\right|, \end{aligned} \tag{26}$$

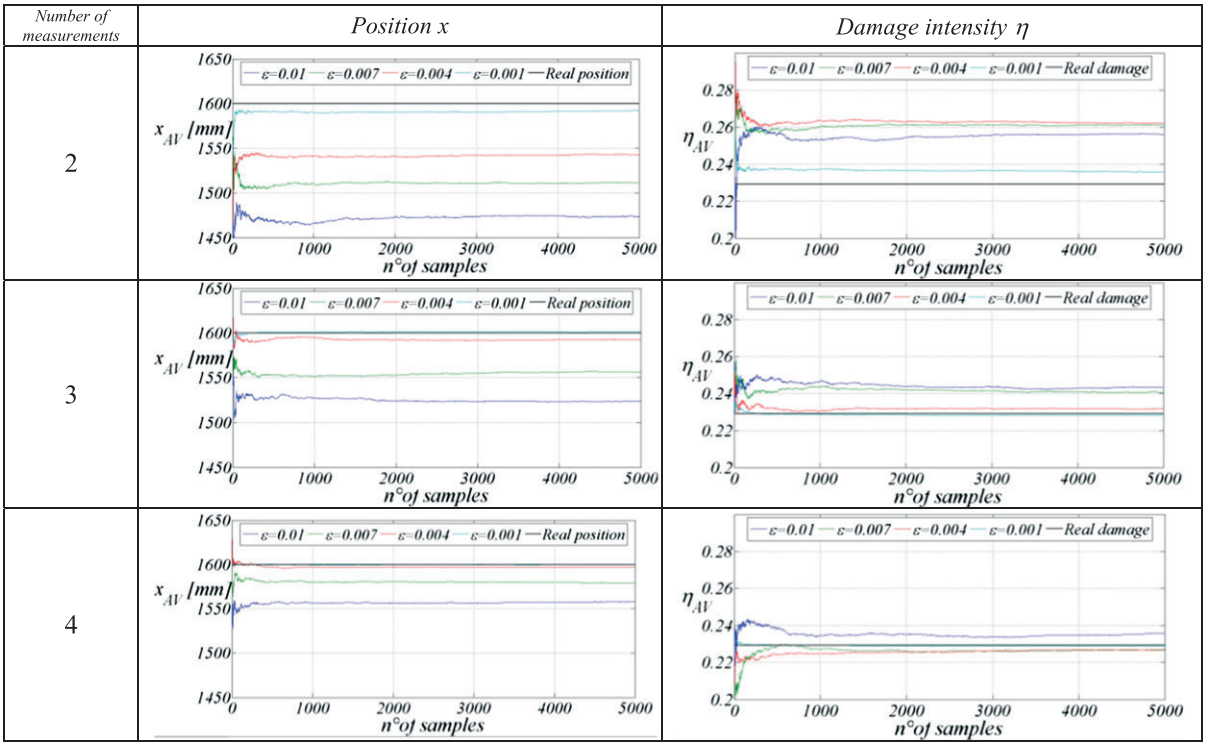

FIGURE 13 Influence of noise: influence of proportional errors on a single-cracked beam

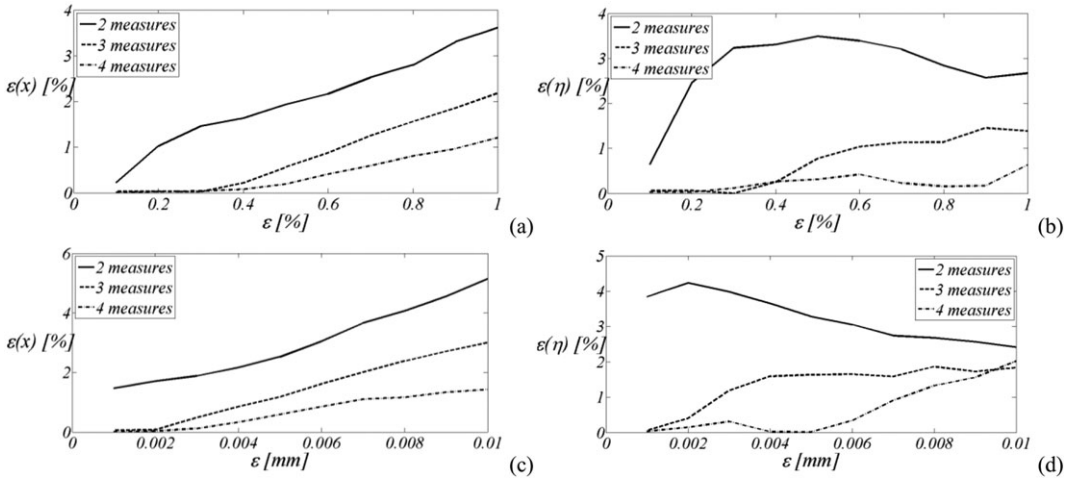

FIGURE 14 Influence of noise—error in the identified values versus error in the measurements: (a) crack location and (b) depth considering noise proportional to the measurements and (c) crack location and (d) depth considering noise with absolute errors

where x_i^r, x_i^{id} represent the real and identified locations of the ith crack, respectively, and η_i^r, η_i^{id} represent the real and identified depths of the ith crack, respectively.

In the following, in order to assess the propagation of the errors along the beam, the double-cracked beam is considered (Figure 12b). Four measurements for each segment are considered, at the abscissae 350, 700, 1,150, 1,400, 1,700, 1,900, 2,100, 2,300, 2,700, 2,900, 3,100, and 3,300 mm.

Again, the two unknown integration constants C_2 and C_4 are equal to 0.007021 and $-1.0417 * 10^{-10}$.

The results relative to the proportional and absolute errors are summarized, considering the mean values after 5,000 samples, in Figure 15. It can be noticed that, for the considered case, higher errors are obtained for the second crack in terms of crack depth but not for the crack location.

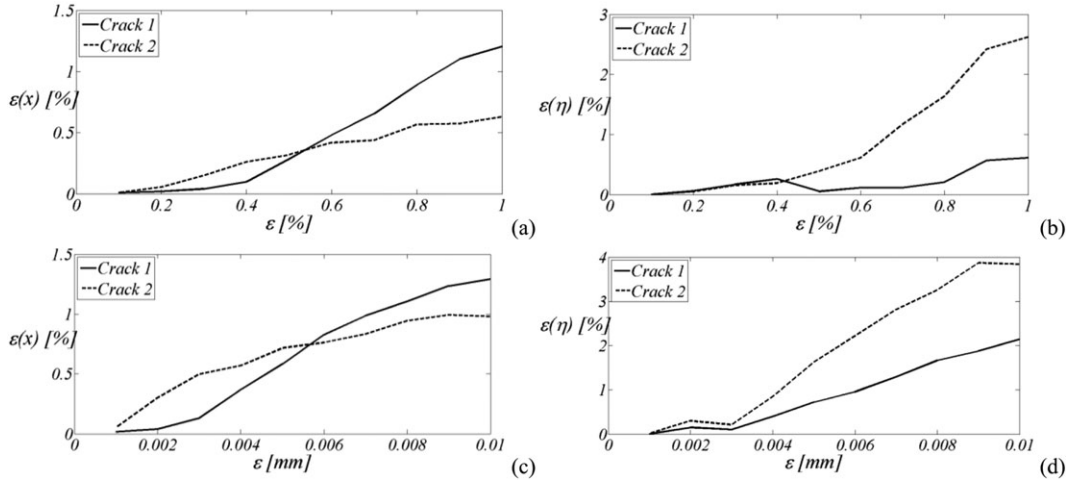

FIGURE 15 Influence of noise—error in the identified values versus error in the measurements: (a) crack location and (b) depth considering noise proportional to the measurements and (c) crack location and (d) depth considering noise with absolute errors

5.4.2 | Crack identification employing additional load scenarios

Alternatively, to increase the number of available data, a possibility is to repeat the experimental test under different load scenarios. In particular, the measurement points are kept at the same locations, and the test can be repeated considering a roving concentrated load.

In the following, the same application reported in Figure 12 is repeated considering the beam subjected to three different load scenarios, namely, a concentrated load of intensity $P = 10{,}000$ N located at the abscissae $x_P = 875$, 1,750, and 2,625 mm. Again, the additional data are treated according to the Moore–Penrose inversion algorithm.

For the single-cracked beam, the measurement points are located at 350, 1,150, 1,900, and 2,300 mm, whereas for the double-cracked beam, two additional stations at 2,900 and 3,300 mm are added. The results are summarized in Figure 16 for the cases of proportional and absolute errors.

For the double-cracked beam reported Figure 12b, the results are summarized in Figure 17 for the cases of proportional and absolute errors.

It is worth to note that the two methods can be combined aiming at increasing the robustness of the procedure; that is, additional measurements can be considered and the test can be repeated for different load scenarios.

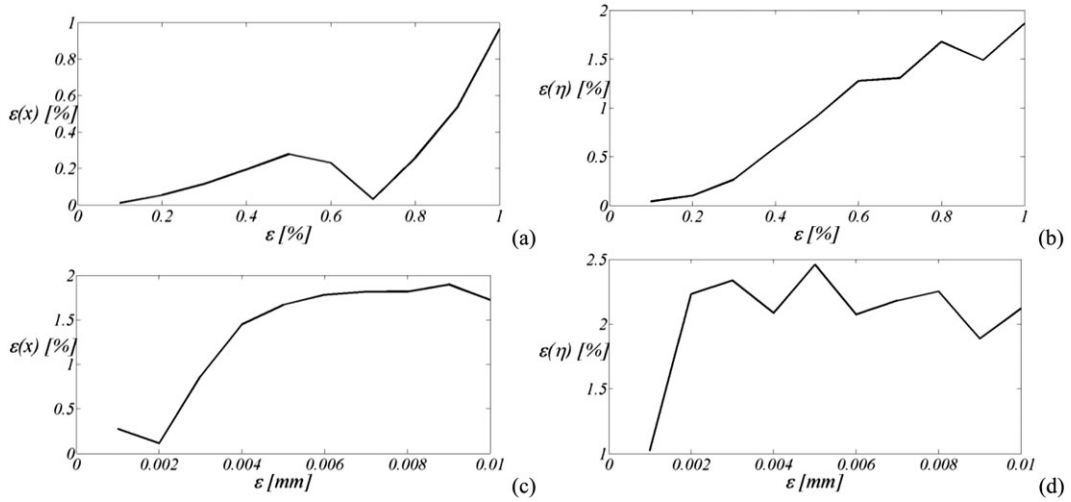

FIGURE 16 Influence of noise—error in the identified values versus error in the measurements: (a) crack location and (b) depth considering noise proportional to the measurements and (c) crack location and (d) depth considering noise with absolute errors

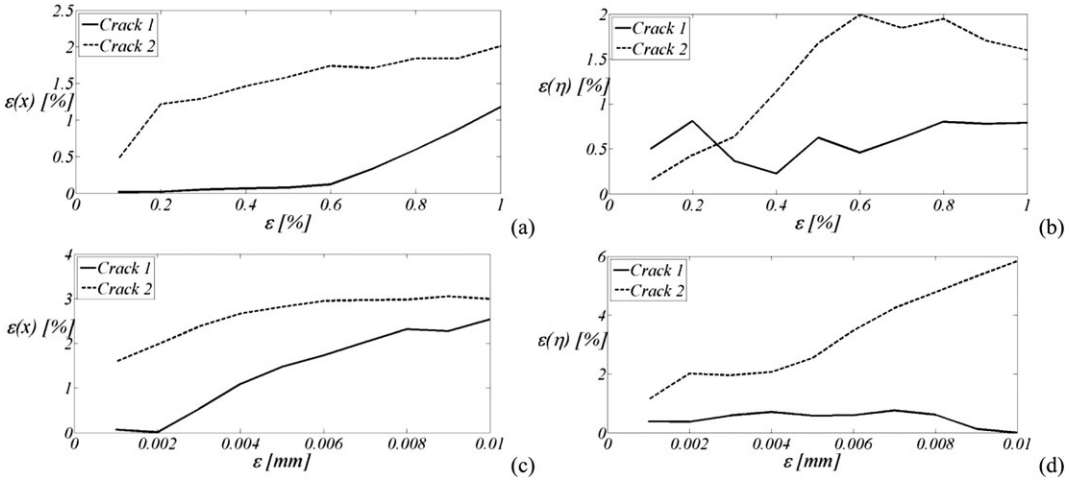

FIGURE 17 Influence of noise—error in the identified values versus error in the measurements: (a) crack location and (b) depth considering noise proportional to the measurements and (c) crack location and (d) depth considering noise with absolute errors

6 | CONCLUSIONS

Very rarely in the literature closed-form expressions for the identification of damage along beam-like structures have been presented. Only recently, explicit solutions have been provided for the case of cracks occurring in beams with specific b.c. in the context of quasi-statically applied loads.

In this work, a different identification procedure leading to alternative explicit expressions for the position and intensity of cracks has been proposed regardless of the number of the cracks and the specific b.c. This has been possible by exploiting the properties of the closed-form solution of a beam with multiple cracks and including the integration constants in the parameters to be identified by the inverse procedure.

The presented procedure seems to be promising in view of its applicability to the case of multiple cracks occurring along frame structures. The procedure is also appealing in view of the possibility to deduce information concerning the occurrence of damage in the portion of the frame that has not been instrumented by monitoring a restricted undamaged portion of the frame.

Several numerical applications and incisive discussions demonstrated the effectiveness of the identification procedure also in presence of noise and provided new findings towards a better understanding of the damage detection problem properties.

ACKNOWLEDGEMENT

The first three authors gratefully acknowledge the financial support of the Ministero dell'Istruzione, dell'Università e della Ricerca (National Research Project PRIN 2015JW9NJT "Advanced mechanical modeling of new materials and structures for the solution of 2020 Horizon challenges").

The fourth author gratefully acknowledges the financial support of the Ministero dell'Istruzione, dell'Università e della Ricerca (National Research Project PRIN 2015 TTJN 95 "Identification and monitoring of complex structural systems").

ORCID

S. Caddemi http://orcid.org/0000-0002-2438-2395

REFERENCES

[1] S. Caddemi, A. Morassi, *Int. J. Solids Struct.* **2007**, *44*(16), 5301.

[2] S. Caddemi, A. Morassi, *J. Eng. Mech-Asce.* **2011**, *137*(2), 113.

[3] B. Biondi, S. Caddemi, *Int. J. Solids Struct.* **2005**, *42*, 3027.

[4] B. Biondi, S. Caddemi, *Eur. J. Mech. A. Solids* **2007**, *26*, 789.
[5] S. Caddemi, I. Caliò, *Int. J. Solids Struct.* **2008**, *45*(16), 1332.
[6] S. Caddemi, I. Caliò, *J. Sound Vib.* **2009**, *327*, 473.
[7] S. Caddemi, I. Caliò, *Comput. Struct.* **2013**, *125*, 137.
[8] S. Caddemi, I. Caliò, *J. Sound Vib.* **2013**, *332*, 3049.
[9] S. Caddemi, I. Caliò, F. Cannizzaro, D. Rapicavoli, *Arch. Appl. Mech.* **2013**, *83*(10), 1451.
[10] S. Caddemi, I. Caliò, *Acta Mech.* **2014**, *225*(11), 3137.
[11] P. Gudmundson, *J. Mech. Phys. Solids* **1982**, *30*(5), 339.
[12] G. Hearn, R. B. Testa, *J. Struct. Eng.* **1991**, *117*(10), 3042.
[13] R. Y. Liang, J. Hu, F. Choy, *J. Eng. Mech-Asce.* **1992**, *118*, 384.
[14] A. Morassi, *J. Sound Vib.* **2001**, *242*(4), 577.
[15] F. Vestroni, D. Capecchi, *J. Eng. Mech-Asce.* **2000**, *126*(7), 761.
[16] Y. Xia, H. Hao, J. M. W. Brownjohn, P. Q. Xia, *Earthq. Eng. Struct. Dyn.* **2002**, *31*, 1053.
[17] H. F. Lam, C. T. Ng, A. Y. T. Leung, *J. Eng. Mech.* **2007**, *134*, 90.
[18] M. Sanayei, O. Onipede, *AIAA J.* **1991**, *29*(7), 1174.
[19] M. Rezaiee-Pajand, M. S. Kazemiyan, S. A. Aftabi, *Mech. Based Des. Struct. Mach.* **2014**, *42*(1), 70.
[20] S. Caddemi, A. Greco, *Comput. Struct.* **2006**, *84*(26–27), 1696.
[21] A. Greco, A. Pau, *Struct. Eng. Mech.* **2011**, *39*(6), 751.
[22] B. K. Raghuprasad, N. Lakshmanan, N. Gopalakrishnan, K. Sathishkumar, R. Sreekala, *Struct. Control Health Monit.* **2013**, *20*(4), 496.
[23] A. Greco, A. Pluchino, F. Cannizzaro, S. Caddemi, I. Caliò, *Appl. Soft. Comput*. **2018**, *64*, 35.
[24] G. R. Irwin, *J. Appl. Mech.* **1957**, *24*, 361.
[25] G. R. Irwin, *Relation of Stresses Near a Crack to the Crack Extension Force*, *9th Congr*. Appl. Mech., Brussels **1957**.
[26] P. F. Rizos, N. Aspragathos, A. D. Dimarogonas, *J. Sound Vib.* **1990**, *138*(3), 381.
[27] G. Gounaris, A. D. Dimarogonas, *Comput. Struct.* **1988**, *28*, 309.
[28] H. Liebowitz, W. D. S. Claus Jr., *Eng. Fract. Mech.* **1968**, *1*, 379.
[29] H. Liebowitz, H. Vanderveldt, D. W. Harris, *Int. J. Solids Struct.* **1967**, *3*, 489.
[30] W. M. Ostachowicz, C. Krawczuk, *J. Sound Vib.* **1991**, *150*(2), 191.
[31] S. A. Paipetis, A. D. Dimarogonas, *Analytical Methods in Rotor Dynamics*, *Elsevier Applied Science*, London **1986**.
[32] P. Gudmnundson, *J. Mech. Phys. Solids* **1983**, *31*, 329.
[33] J. K. Sinha, M. I. Friswell, S. Edwards, *J. Sound Vib.* **2002**, *251*(1), 13.
[34] L. B. Freund, G. Hermann, *J. Appl. Mech.* **1976**, *76*, 112.
[35] S. Caddemi, A. Morassi, *Int. J. Solids Struct.* **2013**, *50*, 944.
[36] H. Hao, Y. Xia, *J. Comput. Civ. Eng.* **2002**, *16*(3), 222.
[37] H. F. Lam, J. H. Yang, *Earthq. Struct.* **2015**, *8*(4), 935.
[38] C. Bilello, *Theoretical and experimental investigation on damaged beams under moving systems. Ph.D. Thesis*, University of Palermo, Italy **2001**.

How to cite this article: Caddemi S, Caliò I, Cannizzaro F, Morassi A. A procedure for the identification of multiple cracks on beams and frames by static measurements. *Struct Control Health Monit*. 2018;e2194. https://doi.org/10.1002/stc.2194